New Journal of Physics
The open-access journal for physics

Nucleation of gold atoms on vanadyl-terminated $V_2O_3(0001)$

N Nilius[1,4], V Brázdová[2], M-V Ganduglia-Pirovano[3,4], V Simic-Milosevic[1], J Sauer[3] and H-F Freund[1]

[1] Fritz-Haber-Institut der MPG, Berlin, Germany
[2] Department of Physics and Astronomy, University College London, London, UK
[3] Humboldt Universität zu Berlin, Berlin, Germany
E-mail: nilius@fhi-berlin.mpg.de and vpg@chemie.hu-berlin.de

New Journal of Physics **11** (2009) 093007 (8pp)
Received 20 May 2009
Published 14 September 2009
Online at http://www.njp.org/
doi:10.1088/1367-2630/11/9/093007

Abstract. The adsorption of Au atoms on a vanadyl-terminated V_2O_3 film grown on Au(111) is studied by means of low-temperature STM and DFT + U calculations. The adatoms preferentially bind in an O—Au—O bridge configuration between two adjacent V=O groups. Missing vanadyl groups that have been identified as the characteristic surface defect do not offer an attractive binding environment and are only sparsely occupied with Au. On the other hand, varying concentrations of V_2O_3 bulk defects that modulate the oxide electronic structure are found to affect the spatial distribution of Au atoms on the oxide surface.

The binding of metal atoms to oxide surfaces deviates strongly from the well-studied behavior on metals. Whereas metals exhibit a rather homogeneous adsorption landscape due to the high degree of electron delocalization, the binding properties of oxides are often dominated by surface defects [1, 2]. Typical oxide defects, e.g. oxygen vacancies and low-coordinated step and kink sites, offer substantially higher adsorption energies when compared with regular sites, as they expose chemically unsaturated atoms or supply extra electrons for bonding [1, 3]. Not surprisingly, the nucleation of metals usually occurs on defects in the oxide surface [4]–[6]. Also the catalytic activity of metal–oxide systems is in part governed by distinct defect-mediated reaction schemes [7]. From the theoretical point of view, the role of defects in anchoring metal atoms to oxide surfaces is well explored, in particular for O vacancies in MgO [8, 9],

[4] Authors to whom any correspondence should be addressed.

© IOP Publishing Ltd and Deutsche Physikalische Gesellschaft

Al_2O_3 [10], TiO_2 [11] and CeO_2 [12]. The experimental side is less advanced. Only a few studies successfully analyzed the interaction of single adatoms with defined oxide defects and revealed the influence on the electronic structure and charge state of the adsorbate [13]–[15].

This scanning tunneling microscopy (STM) and density functional theory (DFT) study explores the role of surface defects in the adsorption of single Au atoms to a vanadyl-terminated $V_2O_3(0001)$ film grown on Au(111). This oxide belongs to the group of Mott–Hubbard insulators and is characterized by a low-temperature band gap of 0.3–0.7 eV that opens below 150 K [16, 17]. The $V_2O_3(0001)$ surface is either terminated by a bulk-truncated O or V plane in strongly oxidizing or reducing environments, respectively, or exposes a dense layer of vanadyl groups at intermediate O_2 chemical potentials [18]–[21]. The vanadyl termination is chemically inert due to the closed-shell electronic structure of the V═O groups that consist of empty V 3d and filled O 2p states. Consequently, defects in the V═O termination are promising candidates for adsorption events. Intrinsic surface defects in the V═O-terminated $V_2O_3(0001)$ are vacancy sites where one V═O group is missing (referred to as vanadyl defects) [20]. Electron bombardment produces another defect type with only the vanadyl oxygen being detached from the surface (referred to as O defect) [18, 19]. These O defects are usually linked to the catalytic activity of the vanadia surface [22].

In this paper, we demonstrate that intrinsic defects in the vanadia surface are less attractive for binding Au than regular sites, contrary to the generally assumed importance of defects for adsorption on oxide surfaces. This unusual behavior is related to the covalent character of V_2O_3 and the peculiar nature of the V═O termination, which both make V═O defects fundamentally different from O vacancies in ionic oxides [2, 3, 9].

The experiments are performed with an ultra-high vacuum STM operated at 5 K [23]. The local density of sample states (LDOS) is probed with differential conductance (dI/dV) spectroscopy, detecting the harmonic current response to a 10 mV rms bias modulation with the lock-in technique. The oxide is prepared by V deposition from an e-beam evaporator onto sputtered/annealed Au(111) in 2×10^{-7} mbar O_2 at 300 K (atom flux of 0.5 ML min^{-1}). Subsequent annealing to 1000 K for 10 min induces the crystallization of the film, but also stimulates its partial de-wetting from the support. The resulting hexagonal oxide islands have 20–50 nm diameter and 3–5 nm height and are delimited by flat (0001)-oriented top facets. Single Au atoms are deposited from a gold-plated W-filament onto the sample held at 10 K. The hot atoms probe a large number of adsorption sites and are expected to reach their preferred binding configuration before thermalization. Due to the large film thickness, the adatoms experience a bulk-like adsorption environment and the influence of the Au support is small. Spin-polarized DFT + U calculations are performed with the gradient-corrected Perdew–Wang 91 functional and a plane-wave basis set (energy cutoff of 250 eV), as implemented in the VASP code [24, 25]. The V-$(2 \times 2)V_2O_3(0001)$ surface is modeled with four (V—O_3—V) tri-layers, according to a $V_{32}O_{48}$ stoichiometry. The V planes are stacked in anti-ferromagnetic order. The U parameter is set as 2.5 eV, which opens a band gap of 1.0 eV in the oxide LDOS. The Brillouin zone is sampled using a $(2 \times 2 \times 1)$ k-point mesh.

Figure 1 shows an overview STM image of a single V_2O_3 grain after Au deposition. The surface is covered with a hexagonal array of protrusions of ∼5 Å lattice constant, being attributed to the (1×1) V═O termination of V_2O_3 [18]–[20]. The dark spots that decorate 5–7% of the lattice sites are either oxygen or vanadyl defects; however, their true nature is not known at this stage. Several gold-related features are detected on the surface. The majority species is imaged as a bright protrusion of 0.9–1.1 Å height and assigned to Au monomers (referred

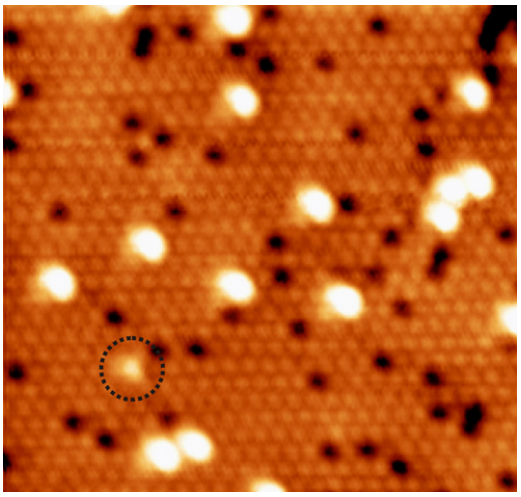

Figure 1. STM image of the vanadyl-terminated V_2O_3 surface covered with 0.02 ML of Au ($13 \times 13\,nm^2$, -0.9 V). The dark holes are missing V=O groups in the surface. The Au atom marked by a circle is localized in such a vacancy site.

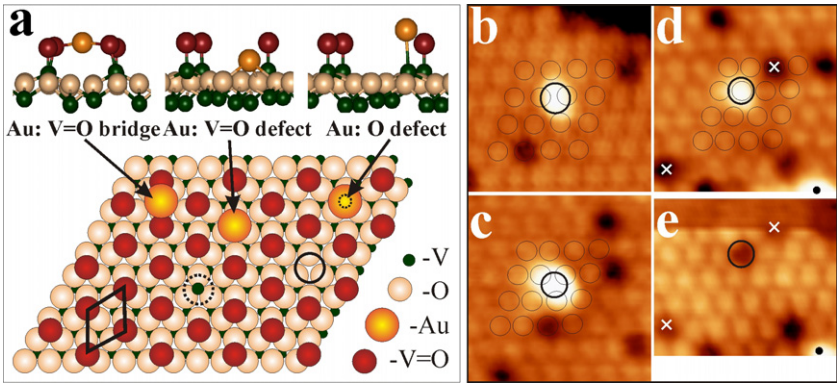

Figure 2. (a) Structure model of V=O-terminated V_2O_3. The diamond depicts the oxide unit cell; the solid and broken circles mark a vanadyl and an oxygen defect, respectively. The insets show the three Au-binding configurations found by DFT. Close-up STM images of Au atoms in (b) a bridge and (c) a hollow position of the V=O lattice ($3.5 \times 3.5\,nm^2$, -0.5 V). The adatom in (d) sits in a V=O vacancy, as demonstrated by removing the atom in a low-bias scan (e). The dot/crosses are guides for the eye to identify similar sites in (d) and (e).

to as Au_r in the following). Their preferred adsorption sites are high-coordinated hollow and bridge sites between the V=O groups, as revealed from the atomically resolved STM images in figures 2(b) and (c). A distinction between the binding configurations is sometimes difficult due to the broad and diffuse appearance of Au-induced maxima in the STM. Approximately, 3% of the adatoms exhibit a reduced height of $\sim$0.5 Å and are referred to as Au_d species in the following (see circle in figure 1). These atoms bind at on-top positions of the V=O lattice (figure 2(d)). As gold adsorption directly atop a V=O group seems to be unlikely, we suggest

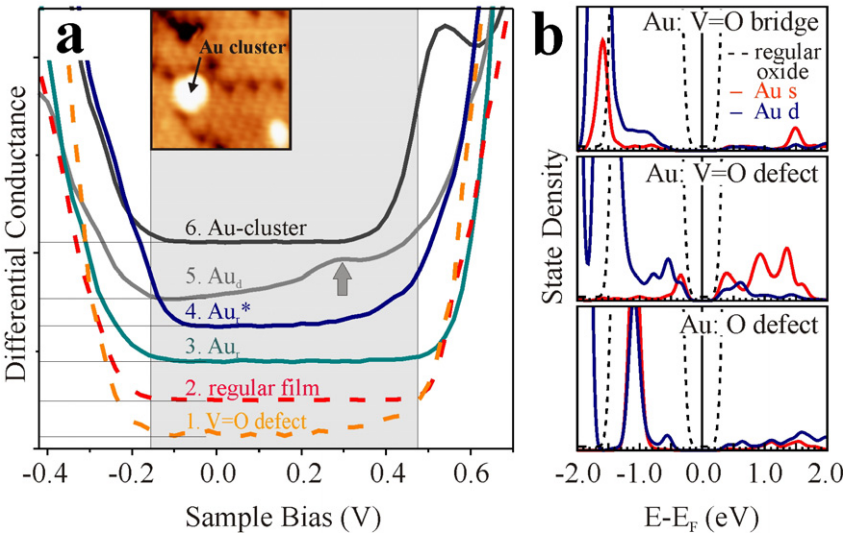

Figure 3. (a) $\mathrm{d}I/\mathrm{d}V$ spectra of a V═O vacancy, an unperturbed oxide region and four different Au species (set point: 0.75 V). The cluster probed in spectrum 6 is shown in the inset ($5 \times 5\,\mathrm{nm}^2$). The V_2O_3 gap region is marked in gray. (b) Calculated LDOS for Au atoms in different binding configurations on the V═O-terminated V_2O_3.

that they occupy defect sites in the vanadyl layer. Experimental evidence for this assumption is obtained from displacing a single $\mathrm{Au_d}$ from its original binding position via scanning at low bias and small tip-sample separation. In the two subsequently taken images in figures 2(d) and (e), the top-bonded species has disappeared and a dark spot becomes visible underneath, indicating a surface defect. The probability for Au atoms to bind to defect positions is surprisingly small, although a large number of such sites seem to be available. Finally, a few larger protrusions are observed on the oxide film, which are attributed to small Au aggregates.

Adatoms in different binding configurations can also be distinguished via their $\mathrm{d}I/\mathrm{d}V$ signature (figure 3(a)). Spectra of the pristine surface are characterized by a region of zero conductance around E_F that marks the correlation band gap in the oxide V 3d states. The gap size varies between 0.5 and 0.7 eV, depending on the preparation conditions and the stoichiometry of the different oxide grains [26]. The gap modulations are introduced by slight changes in the bulk concentration of V versus O vacancies and occur on a length scale of a few nanometers. Surface defects do not affect the gap value and have little influence on the spectral shape (figure 3(a), 1st spectrum) [18]. Also bridge and hollow-bonded $\mathrm{Au_r}$ atoms do not produce new features in the $\mathrm{d}I/\mathrm{d}V$ spectra that remain governed by the V_2O_3 bulk gap (the 3rd spectrum). Only the valence band edge is found to be shifted slightly toward E_F, an effect that is particularly pronounced for a few adatoms termed $\mathrm{Au_r^*}$. In their vicinity, the upshift of the valance band leads to a local decrease of the gap size to 0.4–0.5 eV (the 4th spectrum). The $\mathrm{Au_r}$ and $\mathrm{Au_r^*}$ species are indistinguishable from a purely topographic viewpoint. Defect-bonded $\mathrm{Au_d}$ atoms, on the other hand, exhibit an additional $\mathrm{d}I/\mathrm{d}V$ peak inside the gap region, as demonstrated by the 5th spectrum in figure 3(a). The peak is located at roughly +0.3 V, but slightly varies its position for $\mathrm{Au_d}$ species in different oxide environments. Also small Au clusters show $\mathrm{d}I/\mathrm{d}V$ intensity in the gap region (the 6th spectrum). In contrast to the $\mathrm{Au_d}$ spectra, the maximum

appears close to the conduction-band onset, although its exact energy position depends on the size and shape of a particular aggregate.

The experimental findings are compared to DFT calculations performed for different Au adsorption configurations on regular and defective $V_2O_3(0001)$. The strongest binding takes place on the V terminated surface, where Au binds with 2.33 eV to a V atom. As the V termination does not reflect the experimental situation, this binding scenario is discarded. On the V═O terminated surface, bridge sites between two vanadyl groups have the highest binding potential for Au, while hollow-bonded atoms spontaneously relax toward the adjacent bridge position (figure 2(a)). In this configuration, Au adsorbs with 1.81 eV to two vanadyl oxygen in a nearly linear geometry ($d_{O–Au} = 2.06$ Å). The adsorption is accompanied by a charge transfer out of the Au (Bader charge: $+0.54|e|$). The donated Au electron localizes entirely in the d-shell of one of the two adjacent V atoms, introducing a slight asymmetry between the two V═O groups. In various aspects, the O—Au—O binding configuration resembles the typical building blocks in bulk Au_2O [27]. The binding behavior changes in the presence of surface defects (figure 2(a)). When the complete V═O group is removed, the atom binds with 1.03 eV to a hollow site in the thus exposed bulk-like O layer ($d_{O—Au} = 2.27$Å) and again becomes positively charged ($+0.63|e|$). The weak coupling to the V═O vacancy reflects the high degree of bond saturation in the hexagonal O layer and the electronegative character of both the O and Au atoms. Upon removing only the vanadyl oxygen, the Au binding energy increases to 2.04 eV owing to the strong interaction with the chemically unsaturated V ion ($d_{V—Au} = 2.42$Å). The bond formation is accompanied by a small charge transfer of $-0.36|e|$ toward Au.

The experimental finding that the majority of Au atoms bind to regular V═O lattice sites and the defects remain essentially empty, provides clear evidence that high-binding O defects are not available in the as-prepared film. In this case, the binding to bridge sites is much stronger (1.81 eV) than to the V═O defects (1.03 eV), which is in agreement with observed relative abundance of Au_r versus Au_d species on the surface[5]. Comparing the DFT results to the experimental situation therefore unambiguously identifies the surface defects as V═O vacancies, in agreement with earlier assumptions in the literature [19, 20, 28]. The energetic preference of 0.78 eV to form bridge-bonded Au_r species would imply an even lower probability to find Au_d atoms in vacancy sites. The experimentally determined value of 3% is thus indicative of a kinetic barrier to form Au_r species that might be related to the required distortion of two V═O groups to accommodate the gold.

The assignment of Au_r and Au_d species to calculated binding sites is further supported by the spectroscopic data. No change in the dI/dV spectra around E_F is detected for Au_r atoms, which is compatible with the calculated LDOS of bridge-bonded species (figure 3(b)). The interaction in this case is mediated by the hybridization between the O 2p states of both V═O groups and the Au 5d and 6s orbitals, leading to new d- and s-derived states at -1.6 and $-1.6/+1.5$ eV, respectively (figure 3(b)). Apparently, no Au-induced state emerges in the V_2O_3 gap, in accordance with the experiment. The Au 5d and 6s hybrid states of the Au_r are not detected in the dI/dV spectra, because they strongly interfere with the bulk vanadia states. Also Au attachment to an O vacancy does not produce states in the band gap, as only a mixed level with V 3d and Au 6s/5d character emerges at -1.2 eV in the calculated LDOS (figure 3(b)). The detection of a gap state for the Au_d species therefore supports the assignment of the underlying

[5] The observation of Au_r species in V═O hollow positions is attributed to an inaccurate determination of the binding site with STM.

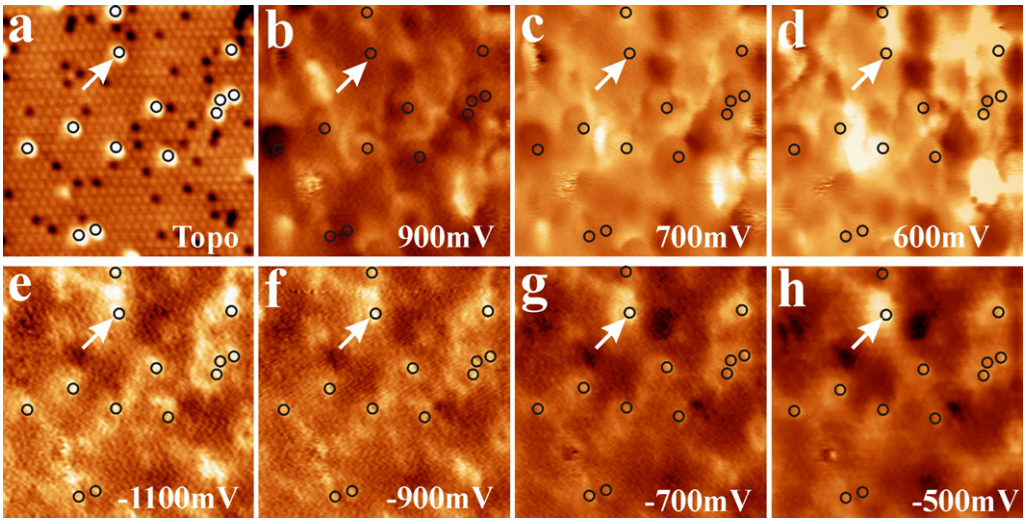

Figure 4. (a) Topographic and (b–h) conductance images of Au atoms on V_2O_3/Au(111) taken as a function of bias ($13 \times 13\ nm^2$). Open circles denote the atom positions, as deduced from (a). The adatoms preferentially bind to regions with high density of filled states. The effect is especially pronounced for the atom marked with an arrow, which refers to an Au_r^* species.

defect to a V=O vacancy. The bond formation in this case involves hybridiziation of the Au 5d and O 2p states, but affects the Au 6s orbital only weakly. As a consequence, the filled and unfilled 6s components remain close to their initial position at E_F and give rise to the dI/dV peak inside the band gap (figure 3(b)). A localization of the Au 6s state in the vicinity of E_F was revealed for Au adsorption to other inert oxide materials as well, e.g. for MgO and Al_2O_3 [9, 10]. The fact that only the unoccupied 6s component of the adatom is detected experimentally might be explained by the asymmetry of the oxide band gap, with the valence band being closer to E_F than the conduction band (see figure 3(a)) [26]. Whereas the valence band onset already covers the filled 6s component, the unfilled level remains visible in the gap region. Finally, the unoccupied dI/dV intensity in the spectra of small Au aggregates indicates the development of quantized electronic states in the cluster volume (figure 3(a), the 6th spectrum). Similar states have been identified previously in other oxide-supported metal clusters [29]. As neither the number of atoms nor their exact configuration can be determined for the given clusters, the quantum nature of the states remains unclear at this stage.

Finally, the nature of the Au_r^* species needs to be discussed. They differ from the regular Au_r in their enhanced conductance at the valence band onset (see figure 3(a), the 4th spectrum). As demonstrated with the dI/dV maps in figure 4, the high conductance at negative bias is not localized at the Au_r^* position (marked by the arrow), but spreads over a certain region around the adatom and, consequently, reflects a property of the oxide film. Apparently, the Au_r^* atoms preferentially bind to surface regions with high dI/dV intensity and hence high state density below E_F. This characteristic, although less pronounced, is also observed for the regular Au_r atoms. For positive bias values, on the other hand, no correlation is revealed between the Au positions and the dI/dV intensity of the surrounding oxide. This observation suggests that Au adsorption is controlled not only by the surface atomic structure, but also by the occupied LDOS in the oxide region below. Such a behavior might be rationalized by the influence of long-range

coupling mechanisms between Au atoms and the oxide film, e.g. polarization and dispersive forces, which are superimposed on the short-ranged chemical interactions. Depending on the electron density available in the bulk, these contributions can locally increase the Au binding strength to the oxide and modulate the potential landscape for adsorption. For V_2O_3/Au(111), the gap size and hence the filled-state density are subject to spatial variations that are introduced by local changes in the oxide stoichiometry [26]. Regions with high LDOS below E_F are hereby assigned to V-poor oxide grains, where the presence of negatively charged acceptor levels leads to an upward bending of the V_2O_3 valence band. According to this picture, the Au_r^* have the same adsorption configuration as the regular Au_r, but experience a slightly higher binding strength due to the larger filled-state density in the oxide below.

In summary, Au atoms on a vanadyl-terminated $V_2O_3(0001)$ surface preferentially bind in a bridge-bonded configuration between two V═O groups, whereas V═O vacancies, being the dominant surface defect, are less attractive for Au adsorption. This surprising result is explained by the fact that the missingV═O group just exposes the inert O layer of bulk V_2O_3 and does not produce a chemically unsaturated defect site. The more reactive oxygen vacancies were not identified in the as-prepared film. The V═O-terminated V_2O_3 surface is therefore a rare example, where surface defects offer lower binding energies than regular sites, in sharp contrast to the generally assumed importance of oxide defects for adsorption.

Acknowledgments

This work was supported by the COST D41 network and the 'Norddeutscher Verbund für Hoch- und Höchstleistungsrechner'.

References

[1] Freund H J and Umbach E (ed) 1993 *Adsorption on Ionic Solids and Thin Films* (Berlin: Springer)
[2] Henrich V E and Cox P A 1994 *The Surface Science of Metal Oxides* (Cambridge: Cambridge University Press)
[3] Shluger A L, Sushko P V and Kantorovich L N 2000 *Phys. Rev.* B **59** 2417
Pacchioni G 2000 *Solid State Sci.* **2** 161
[4] Campbell C T 1997 *Surf. Sci. Rep.* **27** 1
Henry C R 1998 *Surf. Sci. Rep.* **31** 235
[5] Bäumer M and Freund H-J 1999 *Progr. Surf. Sci.* **61** 127
[6] Haas G, Menck A, Brune H, Barth J V, Venables J A and Kern K 2000 *Phys. Rev.* B **61** 11105
[7] Häkkinen H, Abbet S, Sanchez A, Heiz U and Landman U 2003 *Angew. Chem., Int. Ed. Engl.* **42** 1297
[8] Nasluzov V A, Rivanenkov V V, Gordienko A B, Neyman K M, Birkenheuer U and Rösch N 2001 *J. Chem. Phys.* **115** 8157
[9] Del Vitto A, Pacchioni G, Delbecq F O and Sautet P 2005 *J. Phys. Chem.* B **109** 8040
[10] Gomes J R, Illas F, Hernandez N C, Marquez A and Sanz J F 2002 *Phys. Rev.* B **65** 125414
[11] Giordano L, Pacchioni G, Bredow T and Sanz J F 2000 *Surf. Sci.* **471** 21
[12] Zhang C, Michaelides A, King D A and Jenkins S J 2008 *J. Chem. Phys.* **129** 194708
[13] Diebold U 2003 *Surf. Sci. Rep.* **48** 53
[14] Nilius N, Wallis T M and Ho W 2003 *Phys. Rev. Lett.* **90** 046808
[15] Matthey D, Wang J W, Wendt S, Matthiesen J, Schaub R, Laegsgaard E, Hammer B and Besenbacher F 2007 *Science* **315** 1692

[16] Ashkenazi J and Weger M 1973 *Adv. Phys.* **22** 207
Ezhov S Y, Anisimov V I, Khomskii D I and Sawatzky G A 1999 *Phys. Rev. Lett.* **83** 4136
[17] Thomas G A, Rapkine D H, Carter S A, Millis A J, Rosenbaum T F, Metcalf P and Honig J M 1994 *Phys. Rev. Lett.* **73** 1529
[18] Dupuis A C, Abu Haija M, Richter B, Kuhlenbeck H and Freund H-J 2003 *Surf. Sci.* **539** 99
[19] Surnev S, Ramsey M G and Netzer F P 2003 *Prog. Surf. Sci.* **73** 117
[20] Schoiswohl J, Sock M, Surnev S, Ramsey M G, Netzer F P, Kresse G and Andersen J N 2004 *Surf. Sci.* **555** 101
[21] Kresse G, Surnev S, Schoiswohl J and Netzer F 2004 *Surf. Sci.* **555** 118
[22] Abu Haija M, Guimond S, Uhl A, Kuhlenbeck H, Freund H-J, Todorova J K, Ganduglia-Pirovano M V, Döbler J and Sauer J 2006 *Surf. Sci.* **600** 1497
Romanyshyn Y *et al* 2008 *Top. Catal.* **50** 106
[23] Rust H-P, Buisset J, Schweizer E K and Cramer L 1997 *Rev. Sci. Instrum.* **68** 129
[24] Perdew J P *et al* 1992 *Phys. Rev.* B **46** 6671
Kresse G and Furthmüller J 1996 *Comput. Mater. Sci.* **6** 15
[25] Dudarev S L, Botton G A, Savrasov S Y, Humphreys C J and Sutton A P 1998 *Phys. Rev.* B **57** 1505
[26] Simic-Milosevic V, Nilius N, Rust H-P and Freund H-J 2008 *Phys. Rev.* B **77** 125112
[27] Shi R, Asahi C and Stampfl C 2007 *Phys. Rev.* B **75** 205125
[28] Nilius N and Simic-Milosevic V 2008 *J. Phys. Chem.* C **112** 10027
[29] Lin X, Nilius N, Freund H-J, Walter M, Frondelius P, Honkala K and Häkkinen H 2009 *Phys. Rev. Lett.* **102** 206801